Exploration of growth conditions of TaAs Weyl semimetal thin film using pulsed laser deposition

Shien Li(李世恩)[1,2], Zefeng Lin(林泽丰)[2,3], Wei Hu(胡卫)[2], Dayu Yan(闫大禹)[2], Fucong Chen(陈赋聪)[2,3], Xinbo Bai(柏欣博)[2,3], Beiyi Zhu(朱北沂)[2], Jie Yuan(袁洁)[2,4], Youguo Shi(石友国)[2,3,4], Kui Jin(金魁)[2,3,4], Hongming Weng(翁红明)[2,3,4], and Haizhong Guo(郭海中)[1,†]

[1] *Key Laboratory of Materials Physics, Ministry of Education, School of Physics and Microelectronics, Zhengzhou University, Zhengzhou* 450052, *China*
[2] *Beijing National Laboratory for Condensed Matter Physics, Institute of Physics, Chinese Academy of Sciences, Beijing* 100190, *China*
[3] *School of Physical Sciences, University of Chinese Academy of Sciences, Beijing* 100049, *China*
[4] *Songshan Lake Materials Laboratory, Dongguan* 523808, *China*

(Received 9 December 2022; revised manuscript received 20 January 2023; accepted manuscript online 6 February 2023)

TaAs, the first experimentally discovered Weyl semimetal material, has attracted a lot of attention due to its high carrier mobility, high anisotropy, nonmagnetic properties and strong interaction with light. These make it an ideal candidate for the study of Weyl fermions and applications in quantum computation, thermoelectric devices, and photodetection. For further basic physics studies and potential applications, large-size and high-quality TaAs films are urgently needed. However, it is difficult to grow As-stoichiometry TaAs films due to the volatilization of As during the growth. To solve this problem, we attempted to grow TaAs films on different substrates using targets with different As stoichiometric ratios via pulsed laser deposition (PLD). In this work, we found that partial As ions of the GaAs substrate are likely to diffuse into the TaAs films during growth, which was preliminarily confirmed by structural characterization, surface topography and composition analysis. As a result, the As content in the TaAs film was improved and the TaAs phase was achieved. Our work presents an effective method for the fabrication of TaAs films using PLD, enabling possible use of the Weyl semimetal film for functional devices.

Keywords: Weyl semimetal, TaAs film, pulsed laser deposition

PACS: 71.55.Ak, 68.55.–a, 81.15.Fg **DOI:** 10.1088/1674-1056/acb913

1. Introduction

Weyl semimetal (WSM) hosts Weyl fermions as quasiparticles in its low-energy excitation, with and only with Weyl nodes formed by crossing of two non-degenerate bands close enough to the chemical potential.[1–4] TaAs is the first recognized WSM without inversion centers, and also a type of easier-to-grow and nonmagnetic material.[5] Since the discovery of this topological material, it has attracted considerable interest as it shows a series of peculiar phenomena, such as the observation of surface Fermi arcs,[6–12] negative magnetoresistance phenomena due to chiral anomalies,[13] and Weyl nodes.[14]

In addition, TaAs shows high carrier mobility, distinct anisotropy in electrical transport, and strong interaction with light,[15,16] which therefore support the potential applications of TaAs in fields such as quantum computation, photodetection and thermoelectric devices.[17–19] For example, a photodetecting prototype based on the TaAs single crystal has been reported, and TaAs has the advantage of a wide temperature detection region due to its massless chiral Weyl nodes and fairly large absorptance over a broad spectral range.[17] The demonstrated generation of the chiral ultrafast photocurrents of TaAs provides a unique opportunity for novel THz emission with polarization control.[18] It has been reported that TaAs has good thermoelectric properties, which provide potential applications in thermoelectric devices.[19] Therefore, there are many urgent requirements for large-size and high-quality TaAs films for the above-mentioned potential applications.

At present, the TaAs single crystal can be fabricated by chemical vapor transport.[20,21] Recently, TaAs films were successfully grown via molecular beam epitaxy.[22,23] To our knowledge, TaAs thin film has never been reported in the literature with pulsed laser deposition (PLD), which greatly limits its applications for functional devices.[18,24–27] One serious challenge for the film preparation is that TaAs does not melt up to 1400 °C but decomposes before reaching its melting point. In addition, the Ta–As binary system has complicated phase diagrams, including Ta_3As, Ta_2As, Ta_5As_4, TaAs, and $TaAs_2$ phases, which makes it difficult to synthesize the pure TaAs phase, especially in TaAs film.[28,29]

In this work, to explore the optimal growth conditions of the TaAs films by PLD, Ta–As films were grown on various substrates using TaAs targets with different As contents, and their crystalline structures were subsequently characterized. The results reveal that the polycrystalline TaAs films can only be achieved on GaAs substrates, which is likely to provide an effective As-rich atmosphere for TaAs, while the Ta_5As_4 phase prefers to nucleate on other substrates without

†Corresponding author. E-mail: hguo@zzu.edu.cn

© 2023 Chinese Physical Society and IOP Publishing Ltd

the As element. Above all, our study provides a practical approach for the fabrication of the designated films using PLD with certain component-rich substrates, as well as other fabrication methods for special volatile compounds and their related research.

2. Experimental details

First, we tried to fabricate the TaAs films on various small lattice mismatch substrates, such as $SrTiO_3$, $0.7Pb(Mg_{1/3}Nb_{2/3})O_3$–$0.3PbTiO_3$ (PMN–PT), MgF_2, and MgO, using $TaAs_{1+x}$ targets with different As stoichiometric ratios, such as TaAs, $TaAs_{1.1}$, and $TaAs_{1.2}$, via the PLD method. The TaAs films were also grown on the As compound substrate GaAs. All the samples were grown in a high vacuum of 10^{-7} Torr. The deposition temperature was set in the range from 650 °C to 750 °C. The fluence and repetition frequency of the KrF excimer laser ($\lambda = 248$ nm) were ~ 4 J/cm^2 and 5 Hz, respectively. The as-prepared powder of targets with nominal compositions of TaAs, $TaAs_{1.1}$, and $TaAs_{1.2}$ were prepared using the solid-state reaction method, and the actual compositions were confirmed using inductively coupled plasma (ICP) measurement. The targets were synthesized by compressing the powders into the pellets and then sintering at 450 °C for 24 hours in the vacuum furnace with O_2 and H_2O levels that were both less than 10^{-2} Torr. The structural characterization of the TaAs films was performed using a Rigaku SmartLab x-ray diffractometer (XRD). The surface morphology was measured using a Hitachi SU5000 scanning electron microscope (SEM). The composition was analyzed using an energy-dispersive x-ray spectrometer (EDS).

3. Results and discussion

3.1. Film growth conditions

The crystal structure of TaAs is a body-centered tetragonal lattice system with the lattice parameters $a = 3.437$ Å and $c = 11.656$ Å, and the space group is $I41md$ (#109, C_{4v}) (Fig. 1(a)).[13,30–32] First, we chose substrates with similar lattice structures or less mismatch to TaAs, such as $SrTiO_3$ and PMN–PT. The stoichiometric ratio of the TaAs target material is 1:1. Figure 1(d) shows the out-of-plane θ–2θ XRD scans of Ta–As films on $SrTiO_3$, PMN–PT, MgF_2, and MgO substrates. For Ta–As films on $SrTiO_3$ and PMN–PT substrates, diffraction peaks at $2\theta \approx 27.87°$ and 57.58° were observed, indicating (101) and (600) reflections of Ta_5As_4, respectively, while the expected TaAs phase was not detected. According to the phase diagram,[28,33] the appearance of the Ta_5As_4 phase is due to the heavy loss of the As component during the growth process.

To supplement the As content in the films, As-rich targets were used. Figure 1(e) shows the out-of-plane θ–2θ XRD scans of the Ta–As films on the $SrTiO_3$ substrates obtained by the TaAs, $TaAs_{1.1}$, and $TaAs_{1.2}$ targets, respectively, but the expected TaAs phase was not obtained. During the preparation of the TaAs thin films, the target with the excess As component does not achieve the effect of the As supplementation. If the As component is supplemented by increasing the As ratio of the target, a large excess of the As component is required. However, the As component is easily sublimated, and there is a conflict between the large stoichiometric ratio of the As and the high compactness of the target; therefore, the excess ratio of As in the target is limited.

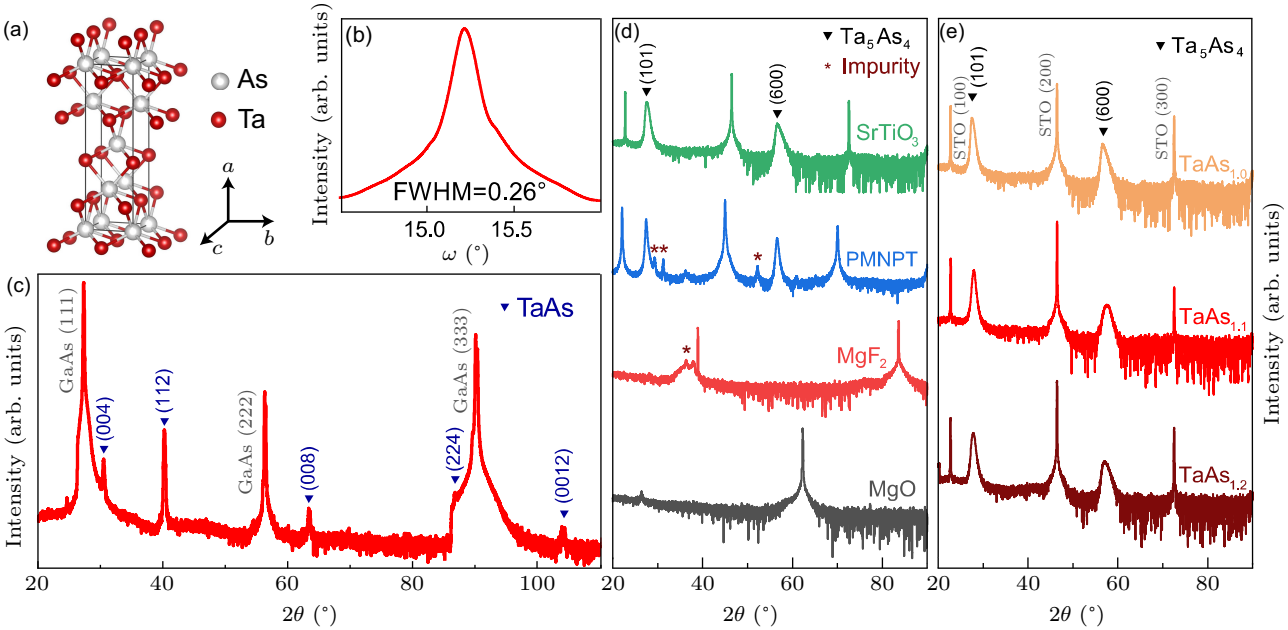


Fig. 1. (a) The body-centered tetragonal structure of TaAs with alternating stacked Ta and As layers. The crystal structure of TaAs does not have space inversion symmetry. (b) The x-ray rocking curve of (004) reflections of the TaAs films, showing a full width half maximum of 0.26°. The θ–2θ XRD scans of (c) the TaAs film on the GaAs substrate, (d) the Ta_5As_4 films on the different substrates, and (e) the Ta_5As_4 films using TaAs targets with different As content.

The TaAs films were fabricated on GaAs substrates, which can provide an As-rich environment. Figure 1(c) illustrates the θ–2θ scans of a TaAs film on the GaAs (111) substrates, exhibiting (004), (008), and (112) diffraction peaks belonging to the TaAs phase. The rocking curve of the (004) peak shows a full width half maximum angle of 0.26° (Fig. 1(b)). Subsequently, we successfully fabricated the TaAs phase films with (004), (008), and (112) orientations on the GaAs (100) and (110) substrates using the same preparation conditions. Therefore, the lattice mismatch is probably not the key reason for these observations, while the As component in the substrates may play an important role in the nucleation of the TaAs phase during the film deposition.

3.2. Evaporation of As from the substrate surface

The method of supplementing volatile compounds using substrates containing the same volatile element is a possible solution. It has been reported that the As content in the GaAs substrate decreases after annealing,[34] and a large number of As crystals appear on the surface of the substrate. In addition, various research groups carried out surface morphology characterization of the annealed GaAs substrate and found that the surface of the substrate was reconstructed.[35,36] To explore the changes in the GaAs substrate during the growth of the TaAs films, we annealed the GaAs substrate at the growth temperature (700 °C) in a vacuum environment (10^{-7} Torr). Then, the changes of the surface and composition of the substrates with different annealing time were investigated using SEM and EDS.

The SEM images of Figs. 2(a)–2(d) show that the surface morphology of the substrate changes significantly after annealing for 10 min, 30 min, 60 min, and 90 min under the same conditions. Under the same magnification ratio, the initial size of the triangular cones on the surface is less than 1 μm, and it continues to expand to more than 5 μm with the increase in the annealing time. The EDS images in Fig. 2 show that with the increase in the annealing time, the area of As evaporation on the surface of the GaAs substrate gradually expands. By comparing the SEM and EDS images of the GaAs substrates at different annealing time, we demonstrate that the As content in the GaAs substrate evaporates from the surface of the substrate during the annealing process, which results in triangular cones on the surface of the substrate.

Figure 3 illustrates the out-of-plane θ–2θ XRD scans of the GaAs substrates annealed at different time. For GaAs substrates, the peaks at $2\theta \approx 45.37°$ represent the (220) reflection. It is found that with the increase in the annealing time, the (220) peak of the GaAs substrates gradually decreases and disappears, and the Ga peak appears at 90 min of annealing. The XRD data of the GaAs substrates with the different annealing time confirm our proposal that the As component in the GaAs substrate slowly evaporates under annealing conditions. It is proposed that the migration of the As component from the GaAs substrate to the films during fabrication provides a new approach for the growth of thin films containing volatile components.

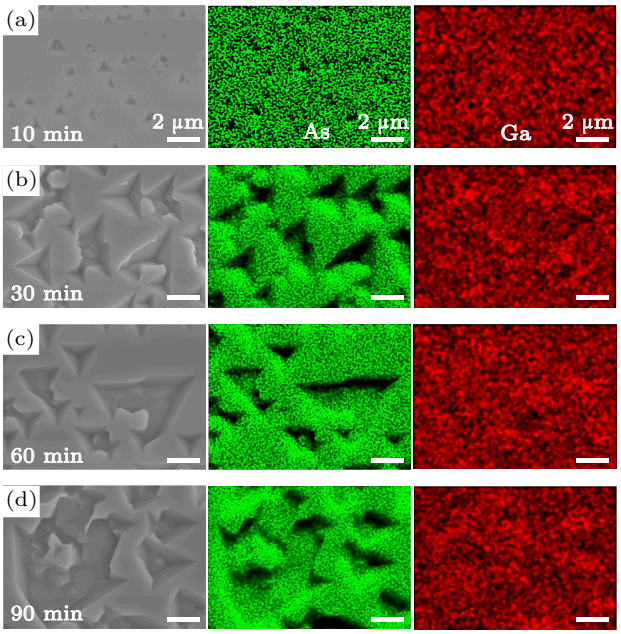


Fig. 2. SEM images and EDS elemental mapping of the TaAs films on the GaAs (111) substrates treated by annealing at 700 °C for (a) 10 min, (b) 30 min, (c) 60 min, and (d) 90 min.

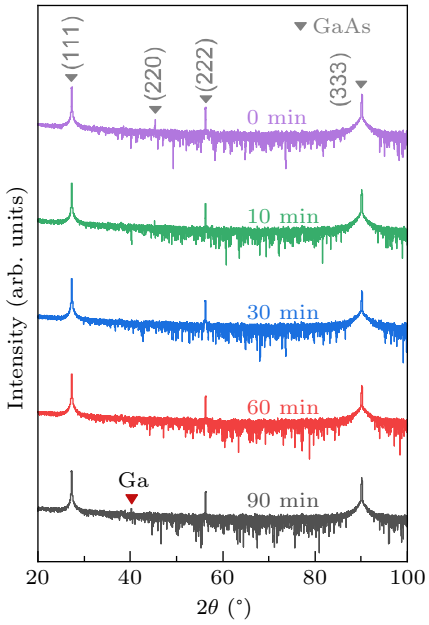


Fig. 3. The θ–2θ XRD scans of the TaAs films on the GaAs (111) substrates for different annealing time.

3.3. Formation mechanism of the TaAs films

We have already found that the As component can evaporate from the GaAs substrate during heating, and we now investigate the formation mechanism of the TaAs thin films. As early as 1993, Han *et al*. reported that the ternary Ta–Ga–As phase could be formed at the interface between Ta and GaAs

thin films due to the diffusion of As components at 850 °C–950 °C.[28] Subsequently, Li *et al.* also found that the $TaAs_2$ phase annealed at 550 °C, and the TaAs, $TaAs_2$, and Cu_3Ga phases annealed at 600 °C were built in the Cu/Ta/GaAs multilayer films because of the percolation of As components.[37] Therefore, we realize that the As component in the GaAs substrate is unstable, and can penetrate to the neighboring Ta layer at high temperature.[38] At present, TaAs film has only been reported to have been prepared successfully on GaAs substrates via molecular beam epitaxy.[22,23]

To explore the TaAs film formation mechanism, we analyze the TaAs thin film using SEM and EDS. The SEM images of Fig. 4(a) show that a large number of irregular crystal grains are randomly scattered on the surface of the TaAs film. In Fig. 4(b), we exhibit the detailed SEM images for the selected area in Fig. 4(a), and we can see that the film has multilayer structures of the crystal grains of 10 nm–100 nm in diameter. The EDS images of Fig. 4(a) display the distribution of As and Ta components on the surface of the film, which is in agreement with the distribution of the Ga component. A detailed analysis of the selected region verifies the same conclusion (Fig. 4(b)). Therefore, it can be determined that the crystal grain is from the TaAs phase.

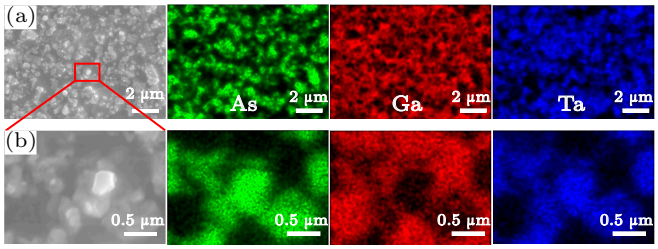


Fig. 4. (a) SEM images and EDS elemental mapping obtained in the TaAs films. (b) Enlarged SEM images and EDS elemental mapping of the red boxed area in (a).

According to the discussion above, one cannot achieve the TaAs film via PLD, even with As-rich TaAs targets. By analyzing the SEM and EDS images of the GaAs substrates for various annealing time, we demonstrate that the As component can evaporate from the GaAs substrate during the annealing process. Therefore, we successfully fabricate the TaAs films using PLD by employing the GaAs substrate to supplement the volatile As component. The bottom-up method to replenish the volatile components from the substrate not only broadens the material types for the film preparation by PLD, but also inspires more ideas for all film fabrication techniques. Further studies are still required to improve the quality of the TaAs films by optimizing the surface treatment of the GaAs substrates.

4. Conclusion

In summary, we report a method for replenishing the volatile As component from the substrate, which enables us to successfully fabricate the TaAs film on the GaAs (111) substrate using PLD. The XRD data indicate that the TaAs film is from the single phase because only (004) and (112) peaks are observed. By studying the SEM and EDS images of the GaAs substrates with different annealing time, we demonstrate that the GaAs substrate plays an important role in the fabrication of the TaAs films, because the As component in the GaAs substrate can diffuse to the surface of the substrate during the annealing process. The method of supplementing volatile components through the substrate not only breaks through the traditional method for increasing the stoichiometric ratio of the volatile component in the target, but also provides possibilities for the preparation of many special films with volatile components by PLD, as well as new inspiration for all film growth methods.

Acknowledgments

We would like to thank Z. Y. Huang, T. X. Liu, J. Xu, Z. Y. Zhao, Y. M. Zhang, Y. J. Shi, Q. Li, and M. J. Cui for helpful discussions. Project supported by the National Key Research and Development Program of China (Grant No. 2021YFA0718700), the National Natural Science Foundation of China (Grant No. 12174347), the Synergetic Extreme Condition User Facility (SECUF), and the Center for Materials Genome.

References

[1] Wan X, Turner A M, Vishwanath A and Savrasov S Y 2011 *Phys. Rev. B* **83** 205101
[2] Xu G, Weng H, Wang Z, Dai X and Fang Z 2011 *Phys. Rev. Lett.* **107** 186806
[3] Bernevig B A 2015 *Nat. Phys.* **11** 698
[4] Weng H, Yu R, Hu X, Dai X and Fang Z 2015 *Adv. Phys.* **64** 227
[5] Weng H, Fang C, Fang Z, Bernevig B A and Dai X 2015 *Phys. Rev. X* **5** 011029
[6] Huang S, Xu S, Belopolski I, Lee C, Chang G, Wang B, Alidoust N, Bian G, Neupane M, Zhang C, Jia S, Bansil A, Lin H and Hasan M 2015 *Nat. Commun.* **6** 7373
[7] Xu S, Belopolski I, Alidoust N, *et al.* 2015 *Science* **349** 613
[8] Lv B, Weng H, Fu B, Wang X, Miao H, Ma J, Richard P, Huang X, Zhao L, Chen G, Fang Z, Dai X, Qian T and Ding H 2015 *Phys. Rev. X* **5** 031013
[9] Xu S, Belopolski I, Sanchez D, *et al.* 2016 *Phys. Rev. Lett.* **116** 096801
[10] Lv B, Muff S, Qian T, Song Z, Nie S, Xu N, Richard P, Matt C, Plumb N, Zhao L, Chen G, Fang Z, Dai X, Dil J H, Mesot J, Shi M, Weng H and Ding H 2015 *Phys. Rev. Lett.* **115** 217601
[11] Yang L, Liu Z, Sun Y, Peng H, Yang H, Zhang T, Zhou B, Zhang Y, Guo Y, Rahn M, Prabhakaran D, Hussain Z, Mo S, Felser C, Yan B and Chen Y 2015 *Nat. Phys.* **11** 879
[12] Liu Z, Yang L, Sun Y, Zhang T, Peng H, Yang H, Chen C, Zhang Y, Guo Y, Prabhakaran D, Schmidt M, Hussain Z, Mo S, Felser C, Yan B and Chen Y 2016 *Nat. Mater.* **15** 27
[13] Huang X, Zhao L, Long Y, Wang P, Chen D, Yang Z, Liang H, Xue M, Weng H, Fang Z, Dai X and Chen G 2015 *Phys. Rev. X* **5** 031023
[14] Lv B, Xu N, Weng H, Ma J, Richard P, Huang X, Zhao L, Chen G, Matt C, Bisti F, Strocov V, Mesot J, Fang Z, Dai X, Qian T, Shi M and Ding H 2015 *Nat. Phys.* **11** 724
[15] Zhang C, Yuan Z, Jiang Q, Tong B, Zhang C, Xie X C and Jia S 2017 *Phys. Rev. B* **95** 085202
[16] Osterhoudt G B, Diebel L K, Gray M J, Yang X, Stanco J, Huang X, Shen B, Ni N, Moll P J W, Ran Y and Burch K S 2019 *Nat. Mater.* **18** 471

[17] Chi S, Li Z, Xie Y, Zhao Y, Wang Z, Li L, Yu H, Wang G, Weng H, Zhang H and Wang J 2018 *Adv. Mater.* **30** 1801372
[18] Gao Y, Kaushik S, Philip E J, Li Z, Qin Y, Liu Y, Zhang W, Su Y, Chen X, Weng H, Kharzeev D E, Liu M and Qi J 2020 *Nat. Commun.* **11** 720
[19] Peng B, Zhang H, Shao H, Lu H, Zhang D W and Zhu H 2016 *Nano Energy* **30** 225
[20] Sankar R, Peramaiyan G, Muthuselvam I P, Xu S, Hasan M Z and Chou F C 2018 *J. Phys.: Condens. Matter* **30** 015803
[21] Li Z, Chen H, Jin S, Gan D, Wang W, Guo L and Chen X 2016 *Cryst. Growth Des.* **16** 1172
[22] Yanez W, Ou Y, Xiao R, Ghosh S, Dwivedi J, Steinebronn E, Richardella A, Mkhoyan K A and Samarth N 2022 *Phys. Rev. Appl.* **18** 054004
[23] Sadowski J, Domagała J Z, Zajkowska W, Kret S, Seredyński B, Gryglas-Borysiewicz M, Ogorzałek Z, Bożek R and Pacuski W 2022 *Cryst. Growth Des.* **22** 6039
[24] Sun K, Sun S, Wei L, Guo C, Tian H, Chen G, Yang H and Li J 2017 *Chin. Phys. Lett.* **34** 117203
[25] Sirica N, Tobey R I, Zhao L, Chen G, Xu B, Yang R, Shen B, Yarotski D A, Bowlan P, Trugman S A, Zhu J, Dai Y, Azad A K, Ni N, Qiu X, Taylor A J and Prasankumar R P 2019 *Phys. Rev. Lett.* **122** 197401
[26] Chen Y, Chen Y, Ning J, Chen L, Zhuang W, He L, Zhang R, Xu Y and Wang X 2020 *Chin. Phys. Lett.* **37** 017104
[27] Gao M, Zhang M, Niu W, Chen Y, Gu M, Wang H, Song F, Wang P, Yan S, Wang F, Wang X, Wang X, Xu Y and Zhang R 2017 *Appl. Phys. Lett* **111** 031906
[28] Han Q and Schmid-Fetzer R 1993 *Mater. Sci. Eng. B* **17** 147
[29] Willerström J O 1984 *J. Less-common Met.* **99** 273
[30] Furuseth S, Selte K and Kjekshus A 1965 *Acta Chem. Scand.* **19** 95
[31] Murray J J, Taylor J B, Calvert L D, Wang Y, Gabe E J, Despault J G 1976 *J. Less-common Met.* **46** 311
[32] Zhang C, Xu S, Belopolski I, *et al.* 2016 *Nat. Commun.* **7** 10735
[33] Han Q and Schmid-Fetzer R 1994 *Mater. Sci. Eng. B* **22** 147
[34] Campos C E M and Pizani P S 2002 *Appl. Surf. Sci.* **200** 111
[35] Zhang S and Northrup J E 1991 *Phys. Rev. Lett.* **67** 2339
[36] Biegelsen D K, Bringans R D, Northrup J E and Swartz L 1990 *Phys. Rev. B* **41** 5701
[37] Chen C, Chang L, Chang E, Chen S and Chang D 2000 *Appl. Phys. Lett.* **77** 3367
[38] Lahav A and Eizenberg M 1984 *Appl. Phys. Lett.* **45** 256